Journal of Experimental Botany, Vol. 71, No. 19 pp. 5911–5923, 2020
doi:10.1093/jxb/eraa338 Advance Access Publication 3 August 2020

RESEARCH PAPER

SINGLE FLOWER TRUSS and *SELF-PRUNING* signal developmental and metabolic networks to guide cotton architectures

Roisin C. McGarry[1,*,†], Xiaolan Rao[1,2,†], Qiang Li[3,‡], Esther van der Knaap[3] and Brian G. Ayre[1]

[1] BioDiscovery Institute, Department of Biological Sciences, University of North Texas, Denton, TX 76203-5017, USA
[2] College of Life Sciences, Hubei University, Wuhan, 430062, China
[3] Center for Applied Genetic Technologies, College of Agricultural and Environmental Sciences, University of Georgia, Athens, GA 30602, USA

‡Present address: College of Horticultural Science and Engineering, Shandong Agricultural University, Tai'an, China.
†These authors contributed equally to this work.
*Correspondence: Roisin.McGarry@unt.edu

Received 14 July 2020; Editorial decision 9 July 2020; Accepted 14 July 2020

Editor: Robert Sharwood, Australian National University, Australia

Abstract

Patterns of indeterminate and determinate growth specify plant architecture and influence crop productivity. In cotton (*Gossypium hirsutum*), *SINGLE FLOWER TRUSS* (*SFT*) stimulates the transition to flowering and determinate growth, while its closely related antagonist *SELF-PRUNING* (*SP*) maintains meristems in indeterminate states to favor vegetative growth. Overexpressing *GhSFT* while simultaneously silencing *GhSP* produces highly determinate cotton with reduced foliage and synchronous fruiting. These findings suggest that *GhSFT*, *GhSP*, and genes in these signaling networks hold promise for enhancing 'annualized' growth patterns and improving cotton productivity and management. To identify the molecular programs underlying cotton growth habits, we used comparative co-expression networks, differential gene expression, and phenotypic analyses in cotton varieties expressing altered levels of *GhSFT* or *GhSP*. Using multiple cotton and tomato datasets, we identified diverse genetic modules highly correlated with *SFT* or *SP* orthologs which shared related Gene Ontologies in different crop species. Notably, altering *GhSFT* or *GhSP* levels in cotton affected the expression of genes regulating meristem fate and metabolic pathways. Further phenotypic analyses of gene products involved in photosynthesis, secondary metabolism, and cell wall biosynthesis showed that early changes in *GhSFT* and *GhSP* levels profoundly impacted later development in distal tissues. Identifying the molecular underpinnings of GhSFT and GhSP activities emphasizes their broad actions in regulating cotton architecture.

Keywords: Cotton, determinate, indeterminate, RNA-Seq, *SELF-PRUNING*, *SINGLE FLOWER TRUSS*, transcriptomes, WGCNA.

Introduction

Enhancing determinate crop architectures is desirable in agriculture: the domestication of many species led to shorter varieties with favorable flowering times and increased yields (Blackman *et al.*, 2010; Liu *et al.*, 2010; Pin *et al.*, 2010). The tomato (*Solanum lycopersicum*) *SELF-PRUNING* (*SP*) gene is a classic example of an architecture gene that revolutionized commercial crop production. Although appearing as a linear axis of growth, the wild tomato vine is a series of determinate, sympodial shoots of alternating vegetative and reproductive growth (Lifschitz *et al.*, 2006; Shalit *et al.*, 2009). Loss-of-function mutations in *SP* cause accelerated termination of sympodial units, resulting in more determinate, shorter tomato plants with more synchronous flowering and fruit ripening (Lifschitz *et al.*, 2006; Shalit *et al.*, 2009). These attributes were a boon for mechanical harvesting, and the *sp* mutation was introduced into commercial tomato cultivars (Yeager, 1927; Rick, 1978).

The Arabidopsis *SP* homolog, *TERMINAL FLOWER 1* (*TFL1*), similarly controls developmental transitions (Ratcliffe *et al.*, 1998; Hanzawa *et al.*, 2005; Baumann *et al.*, 2015). Loss-of-function *Attfl1* mutants flower early and produce a terminal flower in long-day photoperiods (Shannon and Meeks-Wagner 1991), whereas ectopic *AtTFL1* expression extends vegetative and reproductive phases and inhibits the formation of floral meristems (Ratcliffe *et al.*, 1998; Hanzawa *et al.*, 2005; Baumann *et al.*, 2015). *TFL1* belong to the *CENTRORADIALIS/TERMINAL FLOWER 1/SELF-PRUNING* (*CETS*) gene family. FLOWERING LOCUS T (FT), encoding the long-distance flowering signal florigen, is a CETS protein with function antagonistic to TFL1 (Hanzawa *et al.*, 2005; Ahn *et al.*, 2006; Jaeger and Wigge, 2007; Ho and Weigel, 2014; Wang *et al.*, 2015). In long-day conditions, *AtFT* is expressed in the companion cells of the leaf phloem, and the protein moves through the vasculature to meristems. AtFT and AtTFL1 bind the meristem-localized transcription factor FD to activate or repress, respectively, expression of floral meristem identity genes (Abe *et al.*, 2005; Wigge *et al.*, 2005; Hanano and Goto, 2011; Taoka *et al.*, 2011). Consequently, the balance of *TFL1* and *FT* expression directly regulates the balance of vegetative to reproductive growth.

In addition to controlling the transition to reproductive growth, *CETS* genes influence other aspects of development. For example, AtFT interacts with BRANCHED1 (BRC1) to control branching from axillary buds (Aguilar-Martínez *et al.*, 2007; Niwa *et al.*, 2013; Ho and Weigel, 2014). *BRC1* encodes a TCP transcription factor, and down-regulation in axillary buds is important for branch outgrowth (Aguilar-Martínez *et al.*, 2007). Binding of BRC1 to FT prevents the premature transition to flowering in the axils (Niwa *et al.*, 2013). The *Slsp* mutation alters polar auxin transport and auxin responses in tomato (Pnueli *et al.*, 2001; Silva *et al.*, 2018), specifically affecting *AUX/IAA* and *ARF* transcript abundance at sympodial meristems (Silva *et al.*, 2018). This suggests that *SP* influences tomato growth patterns by mediating auxin responses. Thus, changes in *CETS* expression may perturb genetic networks to broadly influence developmental patterns.

Cotton (*Gossypium hirsutum* and *G. barbadense*) is the world's most important fiber crop as well as being a source of oilseed and feed. Domesticated cotton is cultivated as a day-neutral annual row crop, but wild progenitors are photoperiodic trees and shrubs, and residual perennial growth traits challenge crop management. The complex shoot architectures of wild and domesticated cotton are regulated by the cotton *FT* and *TFL1* homologs, *SINGLE FLOWER TRUSS* (*SFT*) and *SP*, respectively (McGarry *et al.*, 2016). *GhSFT* overexpression uncoupled flowering from photoperiod and accelerated the transition to flowering such that normal sympodial iterations terminated prematurely with floral clusters; silencing *GhSP* caused the monopodial main stem and all axillary meristems to terminate prematurely with floral buds. Combining *GhSFT* overexpression with *GhSP* silencing yielded highly determinate yet fertile cotton with dramatically less foliage and synchronized flowering and fruiting. These findings suggested that *GhSFT* and *GhSP* navigate meristems between indeterminate vegetative growth and determinate and reproductive growth (McGarry *et al.*, 2016).

To identify the genetic networks specifying cotton growth habits, we used comparative co-expression, transcriptomics, and functional analyses. Distinct clusters of cotton genes were co-expressed with *GhSFT* and *GhSP*, and, remarkably, these shared related ontologies with networks impacting tomato architectures. Using transcriptomics, we determined that *GhSFT*- and *GhSP*-influenced architectures significantly impacted multiple metabolic pathways. We functionally validated the RNA sequencing (RNA-Seq) results by testing the effects of *GhSFT* and *GhSP* levels on the expression of photosynthesis-related genes using quantitative reverse transcription–PCR (RT–qPCR), and on lignin deposition and cell wall biogenesis using microtomy and histochemical staining.

Materials and methods

Plant inoculations and growth conditions

Gossypium hirsutum Texas 701 (TX701) and Delta Pine 61 (DP61) seedlings were germinated in a 25 °C growth chamber under T5 fluorescent lighting and long days (16 h/8 h). At 4 d post-germination, seedlings remained uninoculated, or the cotyledons were infiltrated with *Agrobacterium tumefaciens* GV3101 pMP90 harboring viral constructs. Virus construction and inoculations were as described (McGarry *et al.*, 2016). Disarmed *Cotton leaf crumple virus* (dCLCrV) was used for gene delivery: dCLCrV was included as a control, and dCLCrV:GhSFT was engineered to overexpress *GhSFT*. *Tobacco rattle virus* (TRV) was used for virus-induced gene silencing: TRV was delivered as a control, TRV:GhSFT was used to silence *GhSFT*, and TRV:GhSP silenced *GhSP*. Following inoculations, plants were covered with a dome, incubated at room temperature overnight, and returned to the same 25 °C growth chamber.

Sample collection and library preparation

At 15 days post-inoculation (dpi), apices were excised from inoculated seedlings and uninoculated controls, fixed in acetone with vacuum infiltration, and acetone was changed twice before storing at 4 °C. Acetone-dried apices were trimmed to 5 mm and expanding leaves were removed. Dried samples were frozen in liquid nitrogen, homogenized using a Retsch mill (Retsch GmbH, Haan, Germany), and RNA was isolated by hot borate (Wan and Wilkins 1994) followed by column clean-up (Zymo

Research, Irvine, CA, USA). Expression of *GhSP* and *GhSFT* was determined by RT–qPCR (McGarry *et al.*, 2016). A 2 µg aliquot of total RNA from uninoculated, dCLCrV:GhSFT-, and TRV:GhSP-infected DP61 and TX701 plants was used to prepare Illumina TruSeq Stranded mRNA libraries (Illumina, Inc., San Diego, CA, USA) as per the manufacturer's protocols, with three biological replicates per treatment per accession.

Preparation and analysis of meristem transcriptomes were previously described (Prewitt *et al.*, 2018). Briefly, DP61 and TX701 plants were grown under short (10 h/14 h) or long (16 h/8 h) days, and apices were harvested at different developmental stages. Apices were fixed in acetone, and meristems and flanking leaves were dissected with the aid of an SMZ 1500 stereomicroscope (Nikon, Melville, NY, USA). The developmental stages from which meristems were harvested included: (i) the monopodial main stem from juvenile DP61 (designated 'DJ' in Supplementary Fig. S1 at *JXB* online); (ii) the monopodial main stem from juvenile TX701 ('TJ'); (iii) the adult monopodial main stem from TX701 grown under non-inductive long days (plants were not flowering; 'TLM'); (iv) monopodial lateral branches from TX701 grown under non-inductive long days (plants were not flowering; 'TL20'); (v) the adult monopodial main stem from TX701 grown under inductive short days after the transition to reproductive growth (plants had flowering sympodial branches; 'TSM'); and (vi) adult sympodial fruiting branches from TX701 grown under inductive short days (flowering sympodial branches; 'TS20'). In addition, the two immature leaves flanking each meristem were harvested and analyzed separately ('DJL','TJL','TLML','TL20L','TSML', and 'TS20L'). Each developmental stage was comprised of three biological replicates, and each replicate consisted of four isolated meristems. RNA was extracted, mRNA amplified with the TargetAmp Amplification kit (Epicenter, Madison, WI, USA), and 125 ng of amplified mRNA was used to prepare Illumina TruSeq mRNA stranded libraries (Illumina, Inc.).

Sequencing, read processing, and data analysis

Libraries were sequenced on a HiSeq2000 (the University of Texas Southwestern Genomics Core), and >30 million 50 bp single-end reads were obtained per replicate. Read quality was checked using the FastQC in the Discovery Environment at CyVerse (Goff *et al.*, 2011); the median quality score was ≥35 for 90% of bases in reads. Reads were aligned to the *G. hirsutum* TM1-1 CRI v1_a1 reference genome (Yang *et al.*, 2019) using the Tuxedo pipeline (TopHat v2.0.9 with Bowtie v2.1.0; Trapnell *et al.*, 2009, 2010) available in the Discovery Environment at CyVerse (Goff *et al.*, 2011). Gene FPKM (fragments per kilobase of exon model per million mapped fragments) values as normalized gene expression levels were calculated with Cufflinks v2.1.1. Cuffdiff v2.1.1 was used to determine significant differences in gene expression between pair-wise comparisons using $q \leq 0.05$ where q is the Benjamini–Hochberg correction to reduce false positives. Venn diagrams were constructed in R (R Development Core Team, 2013); enrichment tests for genes up- and down-regulated by treatment but common to both accessions were conducted using Fisher's exact test with Benjamini–Hochberg multiple testing correction ($q \leq 0.1$), and the results were sorted into MapMan bins (Thimm *et al.*, 2004).

Weighted gene co-expression network analysis (WGCNA)

The WGCNA package in R (Zhang and Horvath, 2005; Langfelder and Horvath, 2008) was used to construct networks from cotton (18 apex and 36 meristem samples described above) and tomato (32 stem samples; NCBI GEO accession GSE132280; Shalit-Kaneh *et al.*, 2019). Raw reads from cotton and tomato samples were aligned to the *G. hirsutum* TM-1 TX-JGI assembly v1.0 and annotation v1.1 (Saski *et al.*, 2017) and *Solanum lycopersicum* SL3.0 (Tomato Genome Consortium *et al.*, 2012) reference genomes, respectively, using TopHat/Bowtie (Trapnell *et al.*, 2009). Normalized gene expression levels were based on FPKM values generated through Cufflinks. Expression data were filtered (FPKM value ≥10, and coefficient of variation >100% for cotton and >50% for tomato) and normalized by $\log_2$-transformed FPKM+1 values. The co-expression gene network modules were constructed using the WGCNA step-by-step network construction; the power transformation was set at 6 using the soft-thresholding method, and other parameters remained at the default settings. The association of *SFT* and *SP* genes with co-expression modules was quantified by the correlation between *SFT*/*SP* gene expression and the module eigengene. The Gene Ontology (GO) biological process terms enriched (Benjamini–Hochberg correction, $P<0.05$) in cotton modules were determined using the PhytoMine tool at Phytozome 12 (https://phytozome.jgi.doe.gov) and ShinyGo v0.60 for tomato modules (Ashburner *et al.*, 2000; The Gene Ontology Consortium, 2019). GO terms were summarized using REViGO (Supek *et al.*, 2011). WGCNA was repeated using the *G. hirsutum* CRI v1_a1 reference (Yang *et al.*, 2019), with the power transformation set at 7 and mergeCutHeight at 0.15. The association of *SFT* and *SP* with co-expression modules was quantified, and the enrichment of GO terms ($P<0.05$) was determined using the Cotton Functional Genomics Database (http://www.cottonfgd.org/).

Gene expression validation

Gene expression was validated by RT–qPCR as previously described (McGarry *et al.*, 2016). Primers were designed to anneal near the 3' end of each coding sequence, span an intron, and yield products of ~130 nt (Supplementary Table S1). Amplification was carried out in 10 µl reactions using 10-fold dilutions of cDNA with PowerUp™ SYBR Green Master Mix (Applied Biosystems, Foster City, CA, USA) on a ViiA™7 Real-Time PCR System (Applied Biosystems) with a fast cycle (UDG activation at 50 °C for 2 min, initial denaturation at 95 °C for 2 min, followed by 40 cycles at 95 °C for 1 s and 60 °C for 30 s) and melt curve analysis (95 °C for 15 s, 60 °C for 1 min, and 95°C for 15 s). Target and reference gene amplifications used three biological replicates and two technical replicates. Data were analyzed by the ΔΔCt method using *GhpolyUBQ* as the reference, and gene expression is expressed as fold change relative to uninoculated plants. Variation is expressed as the standard error of the mean.

Tissue sectioning and staining

Stems between nodes four and five were obtained from mature uninoculated, TRV-infected, and TRV:GhSP-infected DP61 plants. Stems were stored in 100% ethanol at 4 °C until sectioned with a Microm HM 650V vibratome (Thermo Scientific, Waltham, MA, USA). Transverse 75 µm thick sections were stained with phloroglucinol, calcafluor white, and 0.1% toluidine blue-O. Autofluorescence of lignin polymers and cellulose deposition detected with calcafluor white were visualized by UV epifluorescence (excitation wavelengths 340–380 nm and emission wavelengths 435–485 nm) using an Eclipse E600 compound microscope (Nikon, Melville, NY, USA) with SPOT Insight 2 CCD camera (Diagnostic Instruments Inc., Sterling Heights, MI, USA) and an X-cite 120 fluor system (Exfo Life Sciences Division, Quebec, Canada). Phloroglucinol and toluidine blue-O staining were visualized by bright field with the same microscope.

Results

Comparative co-expression analysis identifies distinct SFT *and* SP *genetic networks*

Shoot architecture in wild photoperiodic Texas 701 (TX701) and domesticated day-neutral Delta Pine 61 (DP61) cotton is controlled by the complex balance of *GhSFT* to *GhSP* (McGarry *et al.*, 2016). Using virus-mediated transient gene manipulation, we showed that overexpressing *GhSFT* from the dCLCrV vector uncoupled flowering from photoperiod in TX701 and caused sympodial branches to terminate with clusters of flowers instead of initiating the next sympodial unit (McGarry *et al.*, 2016; and included for clarity in Fig. 1). In

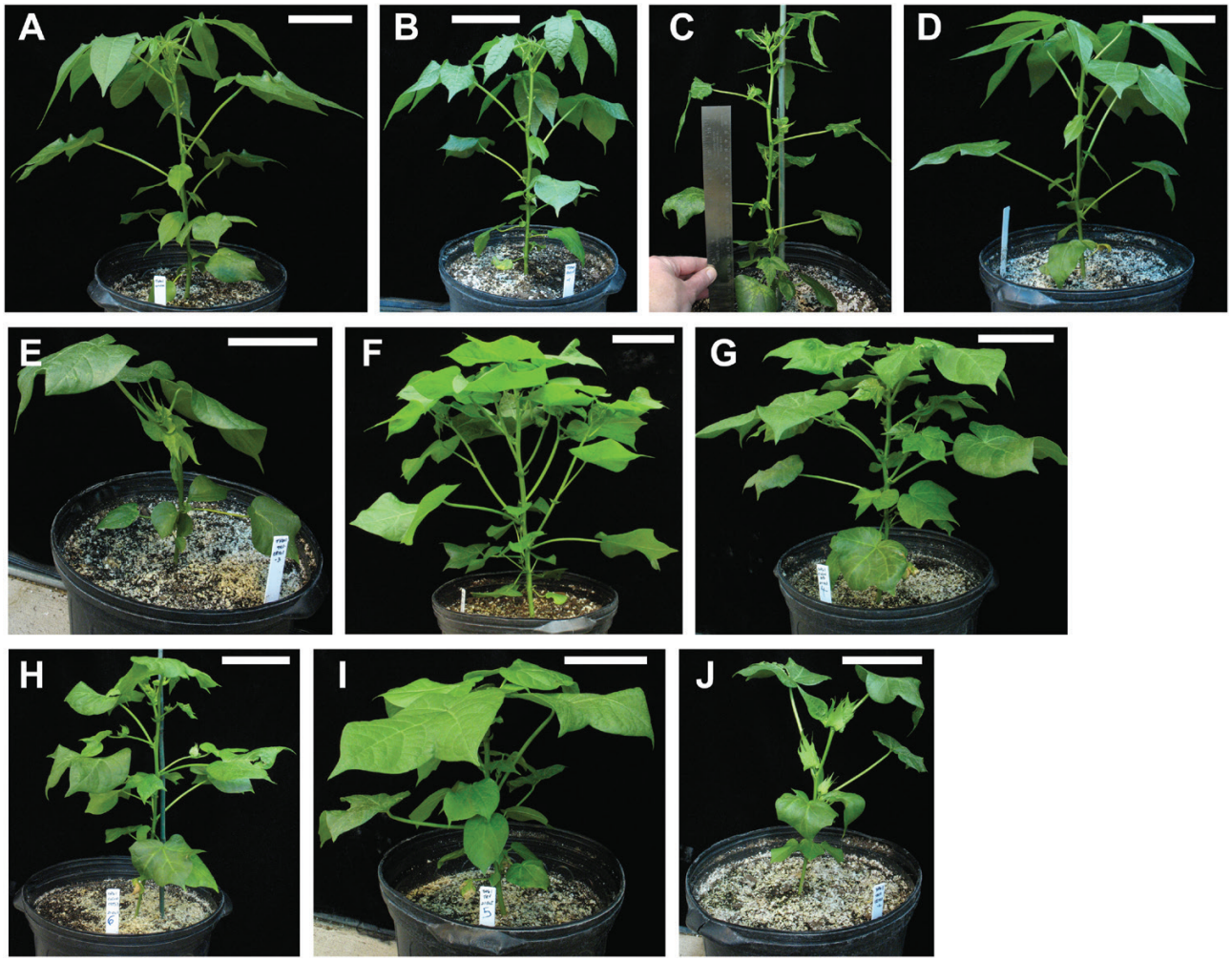

Fig. 1. Changes in *GhSFT* and *GhSP* expression alter cotton architecture. (A–E) TX701 and (F–J) DP61 plants grown under non-inductive long days (16 h/8 h). (A, F) Uninoculated plants; (B, G) plants infected with dCLCrV appear the same as uninoculated plants; (C, H) plants infected with dCLCrV:GhSFT show flowering uncoupled from photoperiod (C) and accelerated transition to determinate growth (C, H); (D, I) plants infected with TRV resemble uninoculated plants; (E, J) plants infected with TRV:GhSP show the main stem terminating growth with a terminal floral bud and all axillary buds terminating with floral buds. Scale bars are 10 cm. (This figure is available in color at *JXB* online.)

day-neutral DP61 infected with dCLCrV:GhSFT, the onset of reproductive growth was accelerated, and fruiting clusters similarly terminated reproductive branches (Fig. 1F–H). In contrast, when *GhSP* was silenced from TRV in photoperiodic and day-neutral lines, the main stem terminated with a flower and all axillary buds terminated with floral buds instead of branches (Fig. 1D, E, I, J). These phenotypes were in striking contrast to uninoculated, dCLCrV-infected, and TRV-infected TX701 and DP61. Changes in *GhSFT* and *GhSP* transcripts, quantified at 15 dpi, correlated with treatments (Supplementary Table S2), suggesting that early regulation of signaling events culminated in the observed phenotypes.

To comprehensively identify cotton genes regulated by *GhSFT* and *GhSP*, we used a WGCNA. From this 'guilt by association' analysis, functional relationships are inferred by identifying groups of genes sharing the same temporal and spatial expression patterns. Fifty-four cotton libraries, comprised of meristems isolated from different developmental stages and photoperiod regimes, and apices with altered *GhSFT* or *GhSP* transcript levels, in TX701 and DP61 were used for co-expression analysis. The expression of *GhSFT* and *GhSP* homeologs, prefixed by 'A' or 'D' to indicate the A and D subgenomes of tetraploid cotton, in each sample is shown in a heat map (Supplementary Fig. S1), with the color intensity reflecting the level of transcript quantified. *GhSFT* was strongly expressed in the apices of dCLCrV:GhSFT-infected plants, whereas *GhSP* transcripts were more abundant in meristems isolated from mature plants (Supplementary Fig. S1). *GhSFT* and *GhSP* expression in each sample is reported as FPKM values (Supplementary Table S2; Prewitt *et al.*, 2018).

A dendrogram of highly interconnected genes was constructed, and 16 modules of co-expressed genes were identified and presented as a color-coded key (Fig. 2A). The correlation between the expression of *GhSFT* and *GhSP* homeologs with each module is shown in the module–trait relationship map, where stronger associations are colored red and weaker associations are blue (Fig. 2B). *GhSFT* and *GhSP* displayed distinct associations with modules. *GhSFT* homeologs associated with the blue module (2956 genes) whereas *GhSP* homeologs strongly associated with turquoise

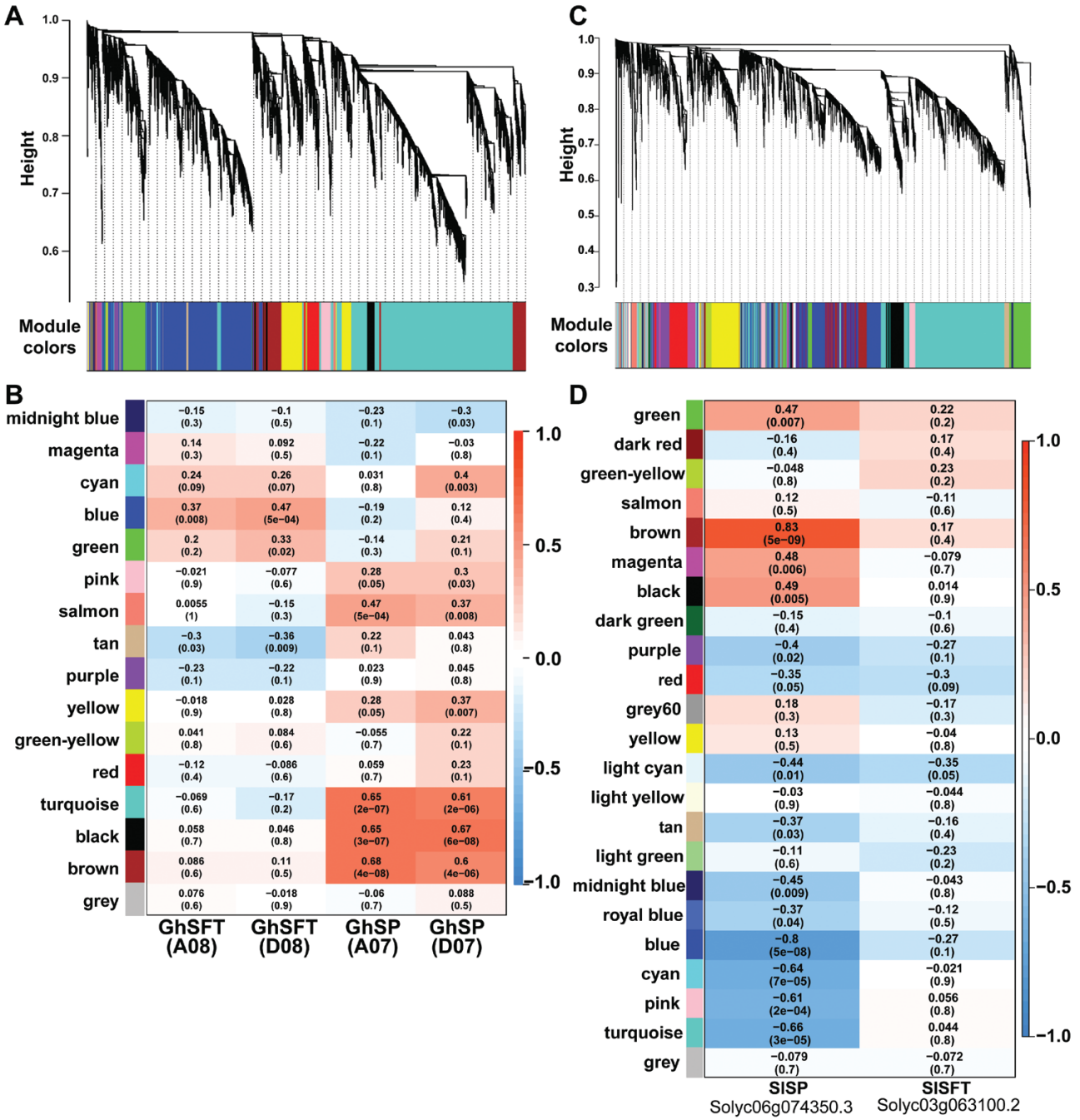

Fig. 2. *SFT* and *SP* are co-expressed with distinct gene clusters. (A) The dendrogram shows co-expressed clusters of genes. Each leaf of the tree represents a gene; interconnected, highly co-expressed genes form the branches of the tree. Sixteen co-expressed clusters or modules were identified from 54 cotton libraries and are represented by the color-coded bar. (B) The correlation of *GhSFT* homeologs, represented as 'A08' and 'D08' to indicate the chromosomes of the A and D subgenomes, and *GhSP* homeologs, represented as 'A07' and 'D07', with each module shown in a heat map. Stronger correlations are colored red; *P*-values are in parentheses. (C) The dendrogram from 32 tomato libraries identified 23 modules of highly co-expressed genes. (D) The module–trait map shows the correlation of *SlSFT* and *SlSP* expression with each module. Stronger correlations are in red; *P*-values are in parentheses.

(4392 genes), black (309 genes), and brown (924 genes) modules, and more moderately with the salmon (67 genes) module. GO terms related to photosynthesis were significantly enriched in the blue (23 genes, $P<0.0015$) and turquoise (41 genes, $P< 2.9\times10^{-15}$) modules (Supplementary Datasets S1–S3). In addition, GO term 'response to auxin' (30 genes, $P<8.8\times10^{-4}$) was overabundant in the turquoise module. The black module was enriched in GO terms related to calcium ion (four genes, $P=0.001$) and H^+ transmembrane transport (eight genes, $P<0.05$). The brown and salmon modules were enriched for GO terms involving the regulation of transcription (99 genes, $P< 3.1\times10^{-20}$ and 15 genes, $P<2.6\times10^{-5}$, respectively), with predicted proteins enriched for NAC, AP2/ERF, and homeobox domains. NAC transcription factors are well-characterized master regulators of lignin and secondary cell wall synthesis (Wang and Dixon, 2012; Taylor-Teeples

et al., 2015) while AP2/ERF and homeobox transcription factors regulate diverse developmental programs (Sluis and Hake, 2015). This analysis emphasizes that *GhSFT* and *GhSP* interact with multiple and diverse clusters of genes, and suggests that *GhSFT* and *GhSP* affect metabolic and developmental patterns through these genetic networks.

The activities of SFT and SP homologs are broadly conserved in other species (Lifschitz *et al.*, 2014), and we questioned if this implied interactions with conserved genetic networks. To test this, we used WGCNA to identify genes co-expressed with *SlSFT* (Solyc03g063100) and *SlSP* (Solyc06g074350) in 32 libraries constructed from mature stems of tomato plants in florigenic or non-florigenic states (Shalit-Kaneh *et al.*, 2019). A dendrogram of 23 color-coded modules was generated (Fig. 2C), and the correlation of *SlSFT* and *SlSP* expression with each was determined (Fig. 2D). As with cotton, *SlSFT* and *SlSP* associated with multiple modules (Supplementary Datasets S4, S5). *SlSP* was strongly co-expressed with brown (794 genes), green (634 genes), black (499 genes), and magenta (293 genes) modules, whereas *SlSFT* weakly associated with brown, green, dark red (48 genes), and green-yellow (142 genes) modules. The brown, black, and green modules were significantly enriched with GO terms related to sucrose transport (three genes, $P<0.05$), cell wall biogenesis (26 genes, $P<1.5\times10^{-15}$), lignin metabolism (10 genes, $P<7.2\times10^{-8}$), and regulation of transcription (58 genes, $P<2.0\times10^{-8}$; Supplementary Datasets S4, S5). While the analyses in cotton and tomato are based on different tissues and maturities, the WGCNA shows that *SFT* and *SP* interact with distinct groups of genes and some of these are involved in related metabolic pathways in cotton and tomato, implying some conservation of *SFT* and *SP* genetic networks in these two species.

Exaggerated changes to GhSFT *or* GhSP *expression perturb genetic networks affecting developmental patterns*

To explore further the pathways involved in cotton architecture regulation, we questioned how changes to *GhSFT* and *GhSP* levels perturbed network dynamics. Differentially expressed genes (DEGs) between uninoculated and dCLCrV:GhSFT-infected, and uninoculated versus TRV:GhSP-infected TX701 and DP61 were analyzed. Because altered expression of *GhSFT* or *GhSP* produced similar phenotypes in wild and domesticated cotton varieties, we focused on transcripts affected by treatment and shared in both genetic backgrounds. The distribution of up- and down-regulated genes was illustrated in Venn diagrams (Fig. 3A, B; Supplementary Table S3). As shown in Fig. 3A, 166 and 549 DEGs were up-regulated when *GhSFT* was overexpressed and when *GhSP* was silenced, respectively, compared with uninoculated TX701 and DP61. A total of 142 and 354 DEGs were down-regulated when *GhSFT* was overexpressed and when *GhSP* was silenced, respectively, compared with uninoculated TX701 and DP61 controls (Fig. 3B).

Changes in *GhSFT* or *GhSP* levels accelerated flowering time in TX701 and DP61: *GhSFT* overexpression impacted sympodial meristems whereas loss of *GhSP* altered the fates of the monopodial apex and axillary meristems (Fig. 1; McGarry *et al.*, 2016). We questioned if these spatial and temporal differences in flowering correlated with differential expression of floral meristem identity genes (Ditta *et al.*, 2004; Bouché *et al.*, 2016). Ectopic *GhSFT* expression did not significantly alter expression of floral meristem identity genes in day-neutral DP61 and photoperiodic TX701 (Table 1). This may reflect the later impact upon sympodial branches and is also consistent with reports that high *SlSFT* is epistatic to mutations in *LEAFY* or *APETALA1* homologs in tomato (Lifschitz *et al.*, 2014). However, *GhSP*-silenced DP61 and TX701 were very determinate and showed increased expression of *LEAFY*, *APETALA1*, and *SEPALLATA4* homologs. Changes in *GhSFT* expression or in other *CETS* genes were not observed in *GhSP*-silenced plants (Supplementary Table S2; McGarry *et al.*, 2016). These results suggest that silencing *GhSP* relieved repression of transcription factors specifying floral meristem fate, and these events correlate positively with earlier flowering time.

Altering GhSFT *and* GhSP *expression magnifies long-term impacts on photosynthesis, secondary metabolism, and cell wall biogenesis*

To test if the DEGs regulated by *GhSFT* or *GhSP* in TX701 and DP61 (Fig. 3A, B) shared coordinated functions, we examined the enrichment of GO terms using MapMan (Thimm *et al.*, 2004). *GhSFT* overexpression or *GhSP* silencing affected multiple metabolic pathways (Fig. 3C). We considered the pathways most likely to impact cotton productivity: photosynthesis, secondary metabolism, and cell wall biogenesis.

Overexpressing *GhSFT* or silencing *GhSP* significantly up-regulated genes involved in photosynthesis ($q<0.0001$; Fig. 3C; Supplementary Table S4). We previously reported that mature source leaves of *GhSP*-silenced cotton achieved and sustained higher levels of photosynthesis, but reasoned that this increased leaf productivity reflected the response of limited source tissues to strong sink demands (McGarry *et al.*, 2016). The enrichment of photosynthesis-related genes at this early developmental stage, that is, at the two-leaf stage and without large sink organs, and in apical tissues protected from photosynthetically active radiation, was surprising. Up-regulation of photosynthetic genes in these young tissues suggests that overexpression of *GhSFT* or silencing *GhSP* predicts a future more determinate plant and a need for greater productivity of the limited vegetative growth. To test if virus load or altered levels of *GhSFT* or *GhSP* influenced expression of photosynthesis-related genes, we analyzed expression of three target genes by RT–qPCR in DP61 plants infected with different viruses. Expression of target genes *Rubisco activase* (*RCA*), *ribulose bisphosphate carboxylase small chain 1B* (*RCS-1B*), and *chaperonin 60 alpha* (*CPN60α*) was quantified relative to the uninoculated controls. As shown in Fig. 4, relative expression of *RCA* and *RCS-1B* was similar to that of controls. Expression of *CPN60α* was enhanced when *GhSFT* or *GhSP* expression was altered, but this was not observed in plants co-infected with dCLCrV:GhSFT and TRV:GhSP. This suggests that *CPN60α* expression responds to changes in *GhSFT* or *GhSP* transcript levels, but not in a dosage-dependent manner, and

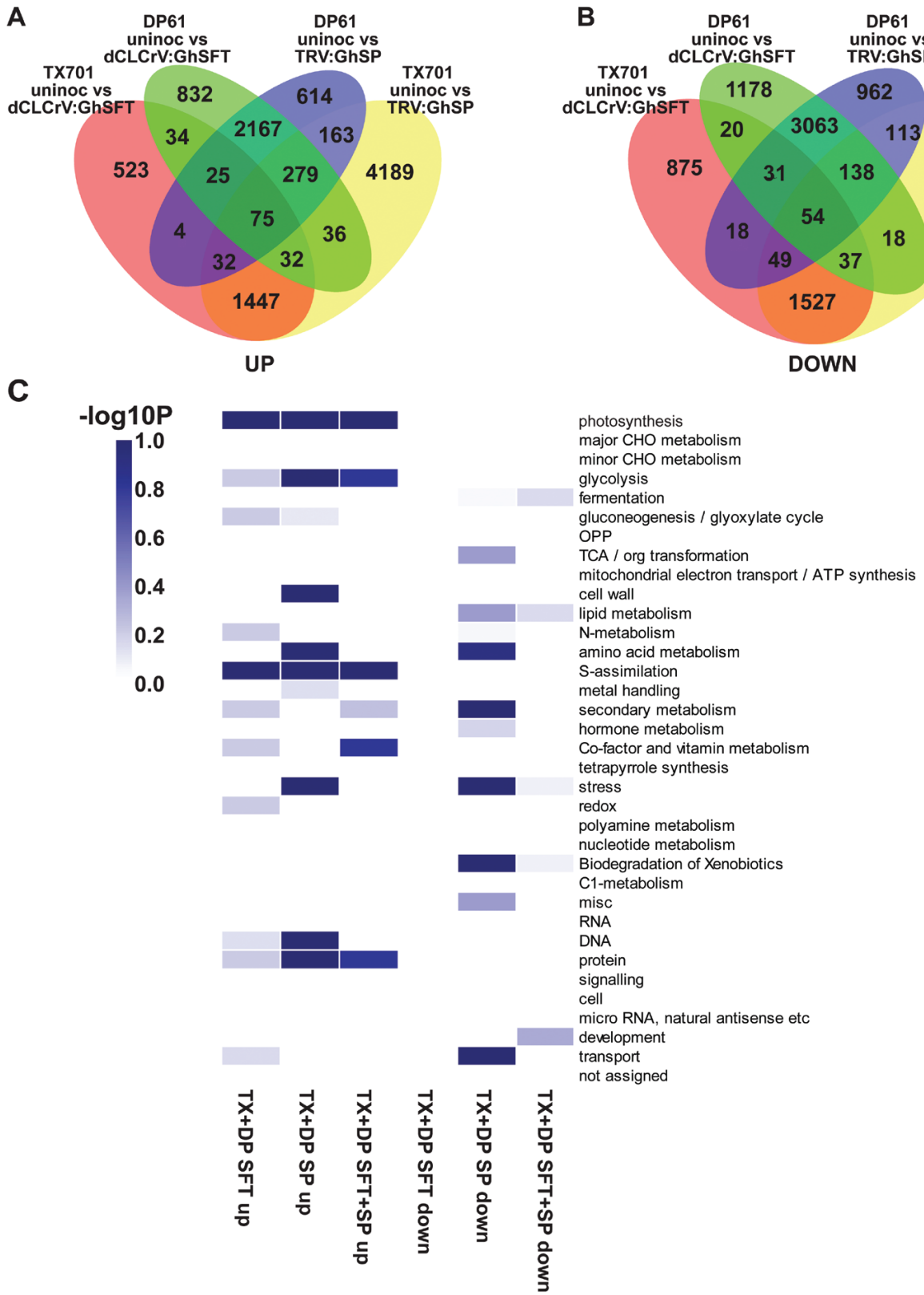

Fig. 3. DEGs shared by treatment between accessions show enrichment in photosynthesis, secondary metabolism, and cell wall-related MapMan bins. (A, B) Pair-wise comparisons of DEGs are illustrated in Venn diagrams. The numbers of genes (A) up-regulated and (B) down-regulated in response to *GhSFT* or *GhSP* manipulation in each accession are indicated. (C) Enrichment analysis of DEGs shared by treatment in both accessions, represented by the overlaps of the Venn diagrams in (A, B), is organized into MapMan bins. The relative expression of genes in each MapMan bin is visualized by a heat map. Shown are the DEGs up- or down-regulated in TX701 and DP61 ('TX+DP') when *GhSFT* is overexpressed ('SFT up' and 'SFT down'), when *GhSP* is silenced ('SP up' and 'SP down'), and when either *GhSFT* or *GhSP* expression is altered ('SFT+SP up' or 'SFT+SP down'). (This figure is available in color at *JXB* online.)

Table 1. Changes in *GhSFT* and *GhSP* expression differentially impact expression of floral meristem identity genes

Gene name	Arabidopsis locus	*G. hirsutum* locus	Sample 1	Sample 2	Fold change	Direction	Total FPKM	*q*-value
LFY	AT5G61850	Gh_A07G051000.1	DP uninoc	DP TRV:GhSP	2.32	UP	14.12	0.001
		Gh_A07G051000.1	TX uninoc	TX TRV:GhSP	4.26	UP	11.65	0.001
		Gh_D07G051800.1	DP uninoc	DP TRV:GhSP	2.80	UP	10.40	0.001
		Gh_D07G051800.1	TX uninoc	TX TRV:GhSP	4.57	UP	9.07	0.001
AP1	AT1G69120	Gh_D13G093100.1	DP uninoc	DP TRV:GhSP	5.30	UP	7.69	0.001
		Gh_D13G093100.1	TX uninoc	TX TRV:GhSP	70.22	UP	4.96	0.029
SEP4	AT2G03710	Gh_A13G085800.1	DP uninoc	DP TRV:GhSP	5.07	UP	5.42	0.001
		Gh_A13G085800.1	TX uninoc	TX TRV:GhSP	14.85	UP	1.76	0.023
		Gh_D13G092900.1	DP uninoc	DP TRV:GhSP	3.44	UP	3.37	0.005
		Gh_D13G092900.1	TX uninoc	TX TRV:GhSP	5.73	UP	1.15	0.030

Shown are the fold changes and FPKM values in the cotton homologs of Arabidopsis floral meristem identity genes identified from the Venn analyses. Significant differences (adjusted *P*-value, $q<0.05$) in pair-wise comparisons between uninoculated ('uninoc') and *GhSP* silencing from TRV ('TRV:GhSP') are reported from DP61 ('DP') and TX701 ('TX'). No significant differences in expression of floral meristem identity genes were observed between uninoculated and *GhSFT*-overexpressing (dCLCrV:GhSFT) DP61 and TX701 plants.
LFY, *LEAFY*; AP1, *APETALA1*; SEP4, *SEPALLATA 4*.

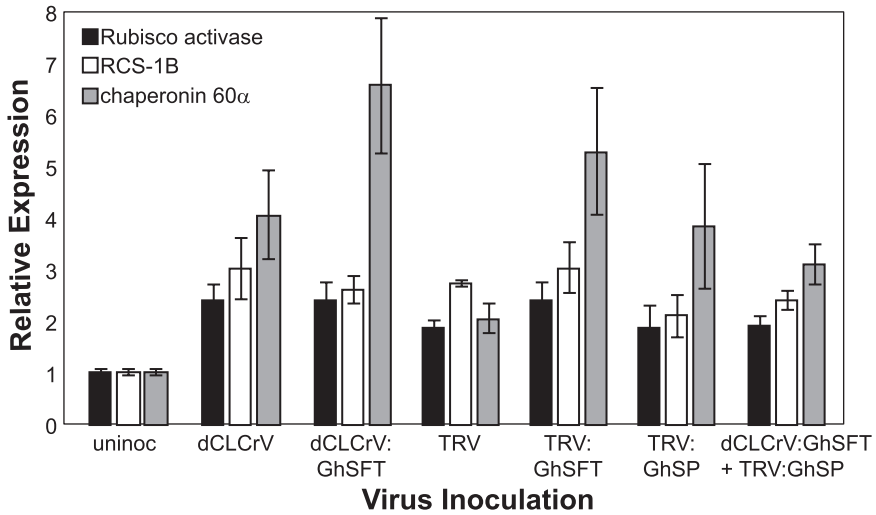

Fig. 4. Expression of photosynthesis-related genes is affected by dCLCrV:GhSFT and TRV:GhSP treatments. The expression of *Rubisco activase* (*RCA*), *ribulose bisphosphate carboxylase small chain 1B* (*RCS-1B*), and *chaperonin 60 alpha* (*CPN60α*) are quantified by RT–qPCR in the apices of DP61 plants infected with viruses altering *GhSFT* and *GhSP* expression. Target gene expression is relative to *GhpolyUBQ*, and fold change is compared against the uninoculated controls. (This figure is available in color at *JXB* online.)

is consistent with the need for greater source leaf productivity later in development.

Silencing *GhSP* significantly suppressed expression of genes involved in phenolic secondary metabolism ($q<0.005$; Fig. 3C). Among the down-regulated transcripts were those encoding laccases, *O*-methyltransferases, hydroxycinnamoyl-CoA shikimate/quinate hydroxycinnamoyl transferases (HCTs), monooxygenases, and flavonol synthase (Table 2; Supplementary Table S5), which are involved in lignin and flavonoid biosynthesis (Zhao *et al.*, 2013; Schuetz *et al.*, 2014). HCTs are lignin biosynthesis enzymes and laccases are lignin-linkage enzymes; the genes encoding these enzymes were co-expressed with *GhSFT* and *GhSP* (Supplementary Datasets S1–S3), and their down-regulation is consistent with reduced lignified cotton stem growth reported in *GhSP*-silenced cotton (McGarry *et al.*, 2016). Importantly, at this early stage of development, these apical tissues are not yet undergoing secondary growth, suggesting that early signals are impacting events later in development.

Reduced lignin in cell walls is compensated by increased production of cell wall carbohydrates (Novaes *et al.*, 2010; Ambavaram *et al.*, 2011). Silencing *GhSP* enhanced expression of cell wall-related genes ($q<0.07$, Fig. 3C), including transcripts encoding expansins and carbohydrate-related enzymes (Table 2; Supplementary Table S6). To test if the deposition of lignin and cell wall carbohydrates changed as a result of *GhSP* silencing, we sectioned stems between nodes four and five from uninoculated, TRV-infected, and TRV:GhSP-infected plants, and used histochemical stains to detect cell wall components. UV light excitation causes autofluorescence of lignins and aromatics; phloroglucinol staining detects cinnamaldehydes in lignin; polychromatic toluidine blue-O appears violet when bound to carboxylated polysaccharides and blue when bound to lignins; and calcafluor white binds cellulose and callose and fluoresces with UV excitation (Mitra and Loqué, 2014). As expected, stem sections from uninoculated and TRV-infected plants were similar: woody transverse sections contained

Table 2. Altering *GhSFT* and *GhSP* impacts expression of cell wall-related genes.

Gene name	Arabidopsis locus	*G. hirsutum* locus	Sample 1	Sample 2	Fold change	Direction	Total FPKM	*q*- value	Function
LAC14	AT5G09360	Gh_A05G234600.1	DP uninoc	DP TRV:GhSP	2.46	DOWN	19.90	0.001	Lignin
		Gh_A05G234600.1	TX uninoc	TX dCLCrV:GhSFT	1.73	DOWN	34.90	0.008	
		Gh_A05G234600.1	TX uninoc	TX TRV:GhSP	1.83	DOWN	34.30	0.002	
		Gh_D05G249500.1	DP uninoc	DP TRV:GhSP	1.90	DOWN	10.13	0.013	
		Gh_D05G249500.1	TX uninoc	TX dCLCrV:GhSFT	1.68	DOWN	14.16	0.022	
		Gh_D05G249500.1	TX uninoc	TX TRV:GhSP	1.77	DOWN	13.89	0.010	
		Gh_D02G076200.1	TX uninoc	TX TRV:GhSP	1.85	DOWN	8.64	0.006	
		Gh_A05G234600.1	DP uninoc	DP dCLCrV:GhSFT	1.58	DOWN	23.07	0.048	
		Gh_A02G073100.1	DP uninoc	DP dCLCrV:GhSFT	2.50	UP	13.07	0.001	
HCT	AT5G48930	Gh_A06G222900.1	DP uninoc	DP TRV:GhSP	1.84	DOWN	51.88	0.006	
		Gh_A06G222900.1	TX uninoc	TX TRV:GhSP	2.10	DOWN	50.88	0.001	
		Gh_A06G222900.1	DP uninoc	DP dCLCrV:GhSFT	1.61	DOWN	54.47	0.032	
		Gh_D06G231100.1	TX uninoc	TX TRV:GhSP	2.15	DOWN	11.75	0.001	
		Gh_D06G229800.4	TX uninoc	TX dCLCrV:GhSFT	3.67	DOWN	5.74	0.017	
ATEXPA4	AT2G39700	Gh_A03G056700.1	DP uninoc	DP TRV:GhSP	1.80	UP	23.16	0.006	Expansin
		Gh_A03G056700.1	DP uninoc	DP dCLCrV:GhSFT	1.59	UP	21.44	0.039	
		Gh_A03G056700.1	TX uninoc	TX TRV:GhSP	1.62	UP	54.59	0.028	
ATEXPA15	AT2G03090	Gh_D13G084100.1	DP uninoc	DP dCLCrV:GhSFT	2.84	UP	27.58	0.001	
		Gh_D13G084100.1	DP uninoc	DP TRV:GhSP	2.33	UP	23.89	0.001	
		Gh_D13G084100.1	TX uninoc	TX TRV:GhSP	1.72	UP	46.33	0.012	
CESA6	AT5G64740	Gh_D05G245100.1	DP uninoc	DP TRV:GhSP	1.70	DOWN	24.85	0.020	Cellulose
		Gh_D05G245100.1	DP uninoc	DP dCLCrV:GhSFT	1.85	DOWN	24.08	0.006	
		Gh_D05G245100.1	TX uninoc	TX TRV:GhSP	1.75	DOWN	14.17	0.012	
XTH	AT3G23730	Gh_A02G021900.1	DP uninoc	DP TRV:GhSP	4.15	DOWN	311.26	0.001	Cell wall
		Gh_A02G021900.1	DP uninoc	DP dCLCrV:GhSFT	7.40	DOWN	284.70	0.001	modification
		Gh_A02G021900.1	TX uninoc	TX dCLCrV:GhSFT	1.72	DOWN	74.16	0.014	
		Gh_D02G024500.1	DP uninoc	DP dTRV:GhSP	2.60	DOWN	262.86	0.001	
		Gh_D02G024500.1	DP uninoc	DP dCLCrV:GhSFT	6.20	DOWN	220.48	0.001	
		Gh_D02G024500.1	TX uninoc	TX dCLCrV:GhSFT	1.81	DOWN	68.89	0.006	
TCH4	AT5G57560	Gh_D02G111600.1	DP uninoc	DP TRV:GhSP	14.39	DOWN	44.26	0.001	
		Gh_D02G111600.1	DP uninoc	DP dCLCrV:GhSFT	16.93	DOWN	43.83	0.001	
		Gh_D02G111600.1	TX uninoc	TX TRV:GhSP	7.29	DOWN	1.46	0.022	

Shown are the fold changes and FPKM values of select cell wall-related genes showing significant differential expression in pair-wise comparisons between uninoculated ('uninoc') and dCLCrV:GhSFT- or TRV:GhSP-infected TX701 ('TX') and DP61 ('DP') cotton. Significant differences (adjusted *P*-value, $q<0.05$) are reported.
LAC14, *LACCASE 14*; HCT, *HYDROXYCINNAMOYL-COA SHIKIMATE/QUINATE HYDROXYCINNAMOYL TRANSFERASE*; ATEXPA4, *EXPANSIN A4*; ATEXPA15, *EXPANSIN A15*; CESA6, *CELLULOSE SYNTHASE 6*; XTH, *XYLOGLUCAN:XYLOGLUCOSYL TRANSFERASE*; TCH4, *TOUCH 4*. The shaded cotton genes overlap with the WGCNA results.

abundant lignin-rich secondary xylem and primary and secondary phloem fiber arrays (Fig. 5A, B, D, E, G, H). Stem sections from uninoculated and TRV-infected plants showed pectin and cellulose in the tissues containing less lignin, mainly in the cortex and periderm (Fig. 5G, H, J, K). The stem sections from *GhSP*-silenced plants, however, had poorly developed secondary xylem, reduced primary phloem fibers, and minimal secondary phloem fibers, all of which contained less lignin than controls, as visualized by UV autofluorescence, phloroglucinol, and toluidine blue-O staining (Fig. 5C, F, I). Additional cell layers extended between the primary phloem fibers and secondary xylem in *GhSP*-silenced stems. The cells in the expanded cortex of *GhSP*-silenced stem sections were large and round, consistent with the up-regulation of expansin genes (Cho and Cosgrove, 2000), and the absence of purple toluidine blue-O staining indicates less pectin relative to controls (compare Fig. 5I with Fig. 5G, H). However, cellulose deposition in *GhSP*-silenced stem sections is more extensive than in controls, continuing through the pith (Fig. 5J, K, L). From the GO and histological analyses, *GhSP* is required for the early expression of genes involved in secondary metabolism and cell wall organization, and, strikingly, the impact of early changes to these genetic pathways continues in distal tissues through development.

Discussion

By investigating early transcriptomic differences in domesticated and wild cottons overexpressing *GhSFT* or silencing *GhSP*, we identified networks of genes correlating with distinct plant architectures. Comparative co-expression and transcriptomic analyses suggest that *SFT* and *SP* networks share similarities between cotton and tomato, and influence diverse metabolic pathways. Experimental testing using virus-based transient expression shows that physiological differences manifesting later in development correlated with early network changes.

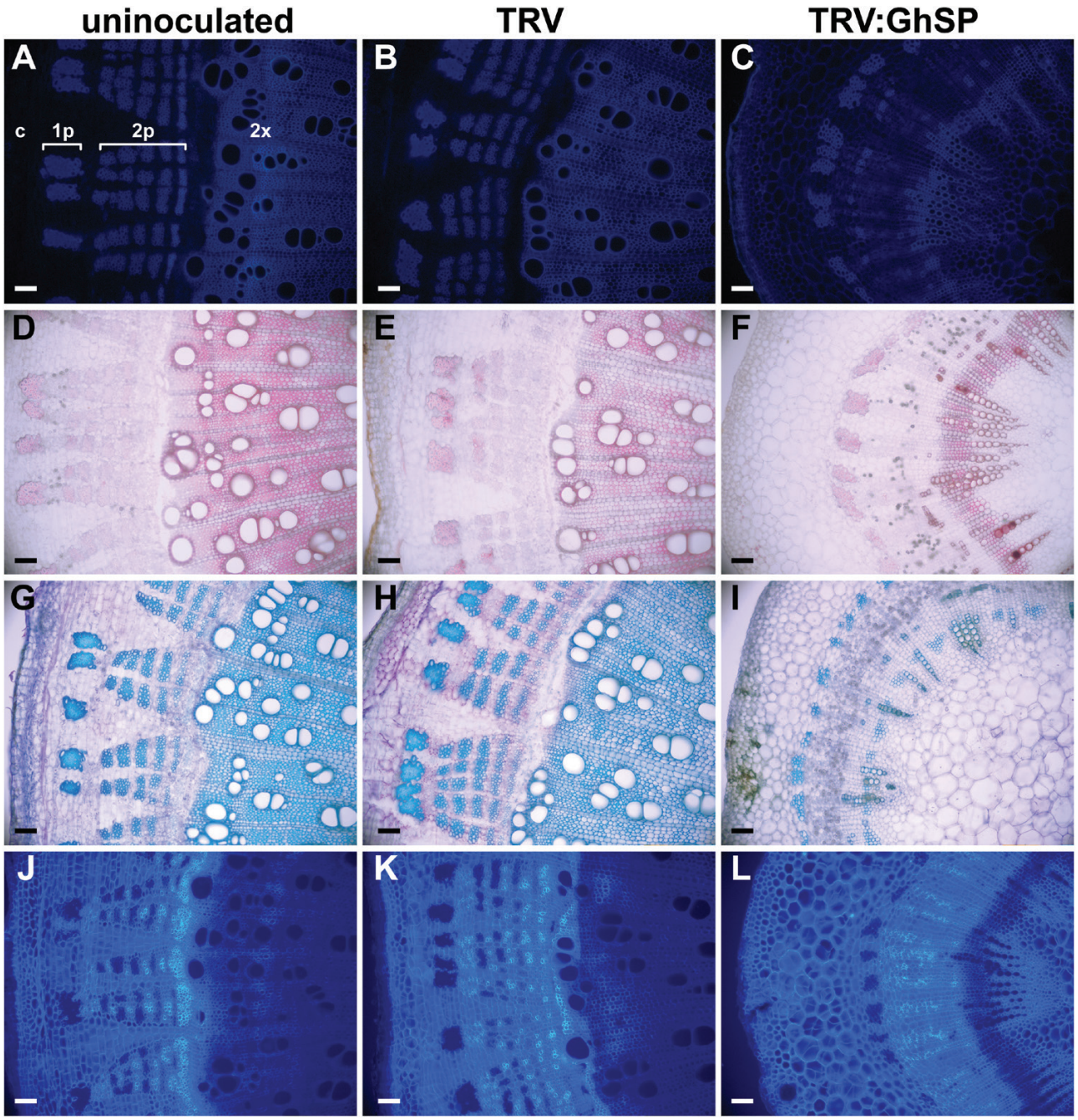

Fig. 5. Silencing *GhSP* alters the composition of cell walls. Transverse 75 μm thick stem sections, obtained between nodes 4 and 5 of the main stem, from mature (~100 d post-germination) uninoculated (A, D, G, J), TRV-infected (B, E, H, K), and TRV:GhSP-infected (C, F, I, L) DP61 plants were visualized using histochemical stains to detect cell wall polymers. UV excitation of lignin polymers is visualized by autofluorescence (A–C); phloroglucinol staining of lignin is observed with bright-field microscopy (D–F); toluidine blue-O staining is blue when bound to lignin and violet when bound to carboxylated polysaccharides (G–I); calcafluor white binds cellulose and callose and fluoresces with UV excitation (J–L). Scale bars are 100 μm. For reference, tissues in (A) are marked with 'c' for cortex, '1p' for primary phloem fibers, '2p' for secondary phloem and secondary phloem fibers, and '2x' for secondary xylem.

GhSFT overexpression and *GhSP* silencing enhanced determinate growth patterns. Our results suggest that *GhSP*, like *AtTFL1*, repressed expression of floral meristem identity genes (Table 1; Ratcliffe *et al.*, 1998; Hanzawa *et al.*, 2005; Baumann *et al.*, 2015). Expression of the same meristem identity genes was not enhanced with high levels of *GhSFT*. This suggested that the determinate growth patterns observed resulted through different signaling pathways. WGCNA further emphasized distinctions in *SFT* and *SP* networks, with co-expressed genes sharing different GOs. Taken together, we show that *GhSFT* and *GhSP* regulate cotton architecture through distinct genetic networks.

Network analyses show that *GhSFT* and *GhSP* affect metabolic pathways and, importantly, we demonstrate that transcriptome changes occurring in young tissues early in development are maintained in different and more mature

organs. *GhSP* expression significantly correlated with the expression of genes encoding transcription factors including NAC, AP2/ERF, and homeodomain proteins. NAC transcription factors are master regulators of secondary cell wall biogenesis (Zhao and Dixon, 2011). Silencing *GhSP* significantly reduced expression of lignin and flavonoid biosynthesis genes while enhancing expression of other cell wall-related genes (Table 2). Together, these findings are consistent with the histological results in mature and distal stem sections: secondary growth was underdeveloped and cells from primary tissues were larger with less lignin and pectin compared with controls (Fig. 5). These results contrast with reports in tomato where overexpressing *SlSFT* enhanced stem vascularization and stimulated expression of secondary cell wall-related genes (Shalit-Kaneh *et al.*, 2019). We did not detect significant enrichment of secondary cell wall-related genes in dCLCrV:GhSFT plants but, with a woody stem, cotton already has high expression of these transcripts. *GhSFT* and *GhSP* transcripts were co-expressed with photosynthesis-related genes, and this finding is supported with MapMan analysis and RT–qPCR shown here, and photosynthesis measurements in leaves of mature plants (McGarry *et al.*, 2016), and is consistent with the co-expression of *SlSFT* and *SlSP* with sucrose transporters in tomato stems. Notably, expression of *CPN60α* was enhanced when *GhSFT* or *GhSP* expression was altered (Fig. 4), consistent with the significant impact this chaperone has for continued plant growth and development. The Arabidopsis *CPN60α* loss-of-function *schlepperless* and temperature-sensitive *CPN60α2* allele show that disruptions to embryonic photosynthesis negatively impact post-germinative growth (Apuya *et al.*, 2001; Sela *et al.*, 2020). Collectively, these findings suggest a conserved mechanism for the determinacy status of the shoot apex to signal future source–sink relationships in developing vegetative (i.e. photosynthetic) organs.

Controlling indeterminate and determinate growth is important for crop productivity and management. Indeed, the compact growth habits of several cotton branching mutants facilitate high-density planting, and these shorter sympodial branches are attributed to mutations in the *GhSP* coding sequence (Si *et al.*, 2018; Chen *et al.*, 2019). Our use of TRV:GhSP-silenced plants allowed us to silence both homeologs simultaneously and thus investigate unique aspects of determinate growth, including termination of the main stem and arrested secondary growth, which are not observed among branching mutants. Our virus-based transient manipulation of *GhSFT* and *GhSP* expression enabled us to query how the balance of these gene products regulates determinate and indeterminate growth patterns in different *G. hirsutum* accessions unamenable to standard transgenic strategies. We show that *GhSFT* and *GhSP* broadly regulate cotton architecture and accomplish this through interactions with multiple and different genetic networks early in development. The coordinated actions of *SFT* and *SP* are needed to specify appropriate building blocks, and fine-tuning their expression offers exciting applications for biotechnology and improving cotton agriculture.

Supplementary data

Supplementary data are available at *JXB* online.

Fig. S1. Sample dendrogram and trait heat maps.

Table S1. Oligonucleotides used for RT-qPCR.

Table S2. Changes in *GhSFT* and *GhSP* expression are quantified and correlate with the different virus treatments.

Table S3. Overlapping TX701 and DP61 genes up- and down-regulated with *GhSFT* and *GhSP* are identified from the Venn diagrams.

Table S4. Significantly differentially expressed genes related to photosynthesis are identified from the MapMan analysis.

Table S5. Significantly differentially expressed genes related to secondary metabolism are identified from the MapMan analysis.

Table S6. Significantly differentially expressed genes related to cell walls are identified from MapMan analysis.

Dataset S1. Cotton module–trait correlation values, Gene Ontology, and predicted protein domain enrichment analyses of cotton gene modules highly co-expressed with *GhSFT* or *GhSP*.

Dataset S2. Cotton module–trait correlation values and enrichment of Gene Ontology of cotton gene modules highly co-expressed with *GhSFT*.

Dataset S3. Cotton module–trait correlation values and enrichment of Gene Ontology of cotton gene modules highly co-expressed with *GhSP*.

Dataset S4, Tomato module–trait correlation values and Gene Ontology of tomato gene modules co-expressed with *SlSFT*.

Dataset S5. Tomato module–trait correlation values and Gene Ontology of tomato modules co-expressed with *SlSP*.

Data availability

Transcriptome data are deposited in the NCBI Gene Expression Omnibus (GSE144546).

Acknowledgements

We thank Dr Richard Dixon for use of the vibratome, Mr Emmanuel Ortiz for instructions on using the vibratome with woody specimens, and Dr Jaime Barros-Rios for suggestions to detect cell wall polymers. This research was supported by United States–Israel Binational Agricultural Research and Development Fund BARD Project number US-4535-12 (BGA) and Cotton Inc. Cooperative Agreement 16-414 (BGA and RCM). The authors have no conflicts of interest to declare.

Author contributions

BGA and RCM designed the experiments; RCM conducted the experiments; RCM, XR, QL, and EvdK analyzed the data; RCM wrote the paper with input from all authors.

References

Abe M, Kobayashi Y, Yamamoto S, Daimon Y, Yamaguchi A, Ikeda Y, Ichinoki H, Notaguchi M, Goto K, Araki T. 2005. FD, a bZIP protein mediating signals from the floral pathway integrator FT at the shoot apex. Science **309**, 1052–1056.

Aguilar-Martínez JA, Poza-Carrión C, Cubas P. 2007. *Arabidopsis BRANCHED1* acts as an integrator of branching signals within axillary buds. The Plant Cell **19**, 458–472.

Ahn JH, Miller D, Winter VJ, Banfield MJ, Lee JH, Yoo SY, Henz SR, Brady RL, Weigel D. 2006. A divergent external loop confers antagonistic activity on floral regulators FT and TFL1. The EMBO Journal **25**, 605–614.

Ambavaram MM, Krishnan A, Trijatmiko KR, Pereira A. 2011. Coordinated activation of cellulose and repression of lignin biosynthesis pathways in rice. Plant Physiology **155**, 916–931.

Apuya NR, Yadegari R, Fischer RL, Harada JJ, Zimmerman JL, Goldberg RB. 2001. The Arabidopsis embryo mutant *schlepperless* has a defect in the *chaperonin-60a* gene. Plant Physiology **126**, 717–730.

Ashburner M, Ball CA, Blake JA, *et al.* 2000. Gene ontology: tool for the unification of biology. The Gene Ontology Consortium. Nature Genetics **25**, 25–29.

Baumann K, Venail J, Berbel A, Domenech MJ, Money T, Conti L, Hanzawa Y, Madueno F, Bradley D. 2015. Changing the spatial pattern of *TFL1* expression reveals its key role in the shoot meristem in controlling Arabidopsis flowering architecture. Journal of Experimental Botany **66**, 4769–4780.

Blackman BK, Strasburg JL, Raduski AR, Michaels SD, Rieseberg LH. 2010. The role of recently derived *FT* paralogs in sunflower domestication. Current Biology **20**, 629–635.

Bouché F, Lobet G, Tocquin P, Périlleux C. 2016. FLOR-ID: an interactive database of flowering-time gene networks in *Arabidopsis thaliana*. Nucleic Acids Research **44**, D1167–D1171.

Chen W, Yao J, Li Y, *et al.* 2019. *Nulliplex-branch*, a *TERMINAL FLOWER 1* ortholog, controls plant growth habit in cotton. Theoretical and Applied Genetics **132**, 97–112.

Cho HT, Cosgrove DJ. 2000. Altered expression of expansin modulates leaf growth and pedicel abscission in *Arabidopsis thaliana*. Proceedings of the National Academy of Sciences, USA **97**, 9783–9788.

Ditta G, Pinyopich A, Robles P, Pelaz S, Yanofsky MF. 2004. The *SEP4* gene of *Arabidopsis thaliana* functions in floral organ and meristem identity. Current Biology **14**, 1935–1940.

Goff SA, Vaughn M, McKay S, *et al.* 2011. The iPlant collaborative: cyberinfrastructure for plant biology. Frontiers in Plant Science **2**, 34.

Hanano S, Goto K. 2011. Arabidopsis *TERMINAL FLOWER1* is involved in the regulation of flowering time and inflorescence development through transcriptional repression. The Plant Cell **23**, 3172–3184.

Hanzawa Y, Money T, Bradley D. 2005. A single amino acid converts a repressor to an activator of flowering. Proceedings of the National Academy of Sciences, USA **102**, 7748–7753.

Ho WW, Weigel D. 2014. Structural features determining flower-promoting activity of Arabidopsis FLOWERING LOCUS T. The Plant Cell **26**, 552–564.

Jaeger KE, Wigge PA. 2007. FT protein acts as a long-range signal in *Arabidopsis*. Current Biology **17**, 1050–1054.

Langfelder P, Horvath S. 2008. WGCNA: an R package for weighted correlation network analysis. BMC Bioinformatics **9**, 559.

Lifschitz E, Ayre BG, Eshed Y. 2014. Florigen and anti-florigen—a systemic mechanism for coordinating growth and termination in flowering plants. Frontiers in Plant Science **5**, 1–14.

Lifschitz E, Eviatar T, Rozman A, Shalit A, Goldshmidt A, Amsellem Z, Alvarez JP, Eshed Y. 2006. The tomato *FT* ortholog triggers systemic signals that regulate growth and flowering and substitute for diverse environmental stimuli. Proceedings of the National Academy of Sciences, USA **103**, 6398–6403.

Liu B, Watanabe S, Uchiyama T, *et al.* 2010. The soybean stem growth habit gene *Dt1* is an ortholog of Arabidopsis *TERMINAL FLOWER1*. Plant Physiology **153**, 198–210.

McGarry RC, Prewitt SF, Culpepper S, Eshed Y, Lifschitz E, Ayre BG. 2016. Monopodial and sympodial branching architecture in cotton is differentially regulated by the *Gossypium hirsutum SINGLE FLOWER TRUSS* and *SELF-PRUNING* orthologs. New Phytologist **212**, 244–258.

Mitra PP, Loqué D. 2014. Histochemical staining of *Arabidopsis thaliana* secondary cell wall elements. Journal of Visual Experiments **87**, e51381.

Niwa M, Daimon Y, Kurotani K, *et al.* 2013. BRANCHED1 interacts with FLOWERING LOCUS T to repress the floral transition of the axillary meristems in Arabidopsis. The Plant Cell **25**, 1228–1242.

Novaes E, Kirst M, Chiang V, Winter-Sederoff H, Sederoff R. 2010. Lignin and biomass: a negative correlation for wood formation and lignin content in trees. Plant Physiology **154**, 555–561.

Pin PA, Benlloch R, Bonnet D, Wremerth-Weich E, Kraft T, Gielen JJL, Nilsson O. 2010. An antagonistic pair of *FT* homologs mediates the control of flowering time in sugar beet. Science **330**, 1397–1400.

Pnueli L, Gutfinger T, Hareven D, Ben-Naim O, Ron N, Adir N, Lifschitz E. 2001. Tomato SP-interacting proteins define a conserved signaling system that regulates shoot architecture and flowering. The Plant Cell **13**, 2687–2702.

Prewitt SF, Ayre BG, McGarry RC. 2018. Cotton *CENTRORADIALIS/TERMINAL FLOWER 1/SELF-PRUNING* genes functionally diverged to differentially impact plant architecture. Journal of Experimental Botany **69**, 5403–5417.

Ratcliffe OJ, Amaya I, Vincent CA, Rothstein S, Carpenter R, Coen ES, Bradley DJ. 1998. A common mechanism controls the life cycle and architecture of plants. Development **125**, 1609–1615.

R Development Core Team. 2013. R: a language and environment for statistical computing. Vienna, Austria: R Foundation for Statistical Computing.

Rick CM. 1978. The tomato. Scientific American **239**, 76–87.

Saski CA, Scheffler BE, Hulse-Kemp AM, *et al.* 2017. Sub genome anchored physical frameworks of the allotetraploid Upland cotton (*Gossypium hirsutum* L.) genome, and an approach toward reference-grade assemblies of polyploids. Scientific Reports **7**, 15274.

Schuetz M, Benske A, Smith RA, Watanabe Y, Tobimatsu Y, Ralph J, Demura T, Ellis B, Samuels AL. 2014. Laccases direct lignification in the discrete secondary cell wall domains of protoxylem. Plant Physiology **166**, 798–807.

Sela A, Piskurewicz U, Megies C, Mène-Saffrané L, Finazzi G, Lopez-Molina L. 2020. Embryonic photosynthesis affects post-germination plant growth. Plant Physiology **182**, 2166–2181.

Shalit A, Rozman A, Goldshmidt A, Alvarez JP, Bowman JL, Eshed Y, Lifschitz E. 2009. The flowering hormone florigen functions as a general systemic regulator of growth and termination. Proceedings of the National Academy of Sciences, USA **106**, 8392–8397.

Shalit-Kaneh A, Eviatar-Ribak T, Horev G, Suss N, Aloni R, Eshed Y, Lifschitz E. 2019. The flowering hormone florigen accelerates secondary cell wall biogenesis to harmonize vascular maturation with reproductive development. Proceedings of the National Academy of Sciences, USA **116**, 16127–16136.

Shannon S, Meeks-Wagner DR. 1991. A mutation in the Arabidopsis *TFL1* gene affects inflorescence meristem development. The Plant Cell **3**, 877–892.

Si Z, Liu H, Zhu J, *et al.* 2018. Mutation of *SELF-PRUNING* homologs in cotton promotes short-branching plant architecture. Journal of Experimental Botany **69**, 2543–2553.

Silva WB, Vicente MH, Robledo JM, Reartes DS, Ferrari RC, Bianchetti R, Araújo WL, Freschi L, Peres LEP, Zsögön A. 2018. SELF-PRUNING acts synergistically with DIAGEOTROPICA to guide auxin responses and proper growth form. Plant Physiology **176**, 2904–2916.

Sluis A, Hake S. 2015. Organogenesis in plants: initiation and elaboration of leaves. Trends in Genetics **31**, 300–306.

Supek F, Bošnjak M, Škunca N, Šmuc T. 2011. REVIGO summarizes and visualizes long lists of gene ontology terms. PLoS One **6**, e21800.

Taoka K, Ohki I, Tsuji H, *et al.* 2011. 14-3-3 proteins act as intracellular receptors for rice Hd3a florigen. Nature **476**, 332–335.

Taylor-Teeples M, Lin L, de Lucas M, *et al.* 2015. An Arabidopsis gene regulatory network for secondary cell wall synthesis. Nature **517**, 571–575.

The Gene Ontology Consortium. 2019. The gene ontology resource: 20 years and still GOing strong. Nucleic Acids Research **47**, D330–D338.

Thimm O, Bläsing O, Gibon Y, Nagel A, Meyer S, Krüger P, Selbig J, Müller LA, Rhee SY, Stitt M. 2004. MAPMAN: a user-driven tool to display genomics data sets onto diagrams of metabolic pathways and other biological processes. The Plant Journal **37**, 914–939.

Tomato Genome Consortium. 2012. The tomato genome sequence provides insights into fleshy fruit evolution. Nature **485**, 635–641.

Trapnell C, Pachter L, Salzberg SL. 2009. TopHat: discovering splice junctions with RNA-Seq. Bioinformatics **25**, 1105–1111.

Trapnell C, Williams BA, Pertea G, Mortazavi A, Kwan G, van Baren MJ, Salzberg SL, Wold BJ, Pachter L. 2010. Transcript assembly and quantification by RNA-Seq reveals unannotated transcripts and isoform switching during cell differentiation. Nature Biotechnology **28**, 511–515.

Wan CY, Wilkins TA. 1994. A modified hot borate method significantly enhances the yield of high-quality RNA from cotton (*Gossypium hirsutum* L.). Analytical Biochemistry **223**, 7–12.

Wang HZ, Dixon RA. 2012. On–off switches for secondary cell wall biosynthesis. Molecular Plant **5**, 297–303.

Wang Z, Zhou Z, Liu Y, *et al.* 2015. Functional evolution of phosphatidylethanolamine binding proteins in soybean and Arabidopsis. The Plant Cell **27**, 323–336.

Wigge PA, Kim MC, Jaeger KE, Busch W, Schmid M, Lohmann JU, Weigel D. 2005. Integration of spatial and temporal information during floral induction in Arabidopsis. Science **309**, 1056–1059.

Yang Z, Ge X, Yang Z, *et al.* 2019. Extensive intraspecific gene order and gene structural variations in upland cotton cultivars. Nature Communications **10**, 2989.

Yeager AF. 1927. Determinate growth in tomato. Journal of Heredity **18**, 263–265.

Zhang BP, Horvath S. 2005. A general framework for weighted gene co-expression network analysis. Statistical Applications in Genetics and Molecular Biology **4**, Article 17.

Zhao Q, Dixon R. 2011. Transcriptional networks for lignin biosynthesis: more complex than we thought? Trends in Plant Science **16**, 227–233.

Zhao Q, Nakashima J, Chen F, Yin Y, Fu C, Yun J, Shao H, Wang X, Wang Z-Y, Dixon RA. 2013. *LACCASE* is necessary and nonredundant with *PEROXIDASE* for lignin polymerization during vascular development in *Arabidopsis*. The Plant Cell **25**, 3976–3987.